A non-isolated PFC bridgeless SEPIC-Cuk converter with adaptive PI controller for induction motor

R. Suguna[1], S. Tamil Selvi[2], K. Mohana Sundaram[3], Pradeep Katta[1]
[1]Department of Electrical and Electronics Engineering, Veltech Hightech Dr. Rangarajan Dr. Sakunthala Engineering College, Chennai, India
[2]Department of Electrical and Electronics Engineering, Sri Sivasubramaniya Nadar College of Engineering, Kalavakkam, India
[3]Department of Electrical and Electronics Engineering, KPR Institute of Engineering and Technology, Coimbatore, India

Article Info

ABSTRACT

In general, the induction motor (IM) is extremely nonlinear in nature and frequency dependent. In most cases, the power generated by the IM has a low power factor (PF), which exhibits detrimental effect on the extent to which the whole transmission and distribution system functions. Since there exists more current harmonics as an outcome of minimized PF, the efficiency of the power system suffers due to transmission line heating and voltage distortion characteristics. Therefore, this paper proposes a power factor correction (PFC) method to overcome the aforementioned issues. Here, by the utilization of AC-DC bridgeless SEPIC-Cuk converter, the power quality is improved by reducing reactive power consumption and enabling better control of voltage and current outputs. To maintain the stable DC link voltage with reduced ripples, the adaptive proportional-integral (PI) controller is used in this work. The three-phase voltage source inverter (VSI) transitioning function is controlled by cascaded fuzzy logic (CFL) controller, which is also utilized for regulating the speed of the three-phase IM. Implementing the proposed control strategy improves power quality significantly by reducing total harmonic distortion (THD). The proposed system is simulated in the MATLAB platform and the attained outcomes, it is clear that the proposed system is highly effective.

Corresponding Author:

R. Suguna
Department of Electrical and Electronics Engineering,
Veltech Hightech Dr Rangarajan Dr Sakunthala Engineering College
Chennai, Tamil Nadu, India
Email: rsuguna016@gmail.com

1. INTRODUCTION

In the industrial sector, induction motors are used in numerous applications due to their characteristics like reduced maintenance, easy operation and robustness. During the operation of induction motor, some harmonic contents are produced which in turn affects the overall system function and this issue is rectified by power factor correction (PFC) method [1]–[4]. Considering the severe PFC requirements for power electronic devices, significant progress has been achieved in the creation of effective PFC converters. Power supply with active power factor correction techniques are required by harmonic rules and standards for electronic equipment [5]. PFC rectifiers are used in a variety of industrial, communications and biomedical applications. Due to their excellent efficiency, bridgeless converter topologies for PFC have grown in significance during the past ten years. In these arrangements, the front-end diode bridge rectifier is not present, which lowers the associated conduction losses [6]–[9].

A full bridge generator using active power factor techniques cannot deliver a significant voltage gain due to the simultaneous operation of three semiconductors switches. Considerable analysis has been carried out developing effective bridgeless PFC circuit topologies in response to these issues [10]. Current in bridgeless PFC circuits passes through the lowest number of switches when contrasted with traditional PFC circuitry. Due to their inexpensive price, uncomplicated circuit and superior functionality in regards to effectiveness and power factor, boost-type circuit configurations are currently used at the front end of the majority of PFC topology [11], [12]. But for applications requiring a wide range of input voltages, the boost converter has poorer efficacy and higher overall harmonic distortion. Numerous researchers have presented PFC topologies based on Cuk [13], SEPIC [14], and buck-boost converters [15], [16]. But the output of these topologies is inverted with high current ripples and high voltage stress. Therefore, a new AC-DC bridgeless SEPIC-Cuk converter is implemented here, which has more benefits including non-inverted output, enhanced efficacy at low input voltage, minimized switch voltage stress and minimized ripples with enhanced PF.

The effectiveness of bridgeless rectifier circuit is enhanced by proportional-integral (PI) controller which is frequently employed in electrical converters due to its reliability under a variety of operational conditions and simplicity in deployment [17]. Sivaramkrishnan *et al.* [18] have presented the PI controller operated with the converter, which is utilized to preserve the DC link voltage constant. To drive the SEPIC converter, Mohanta *et al.* [19] has proposed a better PI controller. However, established PI control gain values display instability, substantial error and delayed dynamic features under a wide range of functioning conditions. Although the fuzzy controller comprises a mathematically complicated architecture, it delivers good dynamical stability with improved capacity to govern linear and non-linear systems. As an outcome, an adaptive PI controller that addresses the drawbacks of both standard and fuzzy controllers has been developed for PFC rectifier regulation in the present research. Several methods have been proposed to regulate the speed of induction motors (IMs), such as PI controller [20] and fuzzy controller [21]. IM speed is controlled by changing the input current. Additionally, there is a necessity for speed control techniques because of issues with voltage source inverter (VSI) dynamics and transitioning effectiveness. To overcome the above issues, the cascaded fuzzy logic controller (FLC) is utilized in this work for efficient speed regulation of three-phase IMs.

As a result, an AC-DC bridgeless SEPIC-Cuk converter is developed in this process that provides enhanced power quality (PQ) with unity PF. An adaptive controller with PI controls the operation of the proposed converter. The speed of three-phase IM is regulated by the deployment of cascaded fuzzy logic (CFL) controller. The recommended system is implemented utilizing MATLAB platform to prove its effectiveness. The attained outcomes show that the presented method has high efficiency with minimized total harmonic distortion (THD).

2. PROPOSED SYSTEM

Figure 1 depicts a schematic depiction of the proposed technique, which includes an adaptive PI controller, an AC-DC bridgeless SEPIC-Cuk converter, and a CFL controller. The suggested converter produces an output voltage with the least number of ripples providing improved power factor correction. The inputs for the adaptive PI controller are the actual and reference voltage, while the optimal output generated is given to the pulse width modulation (PWM) generator, resulting in the gating pulses for converter. The necessary signals are created and delivered to the converters using a PWM generator and real and reference current. This remarkably aids to keep input and output current in-phase with each other. Additionally, since the fluctuation of the load significantly affects the speed of motor operation, the better output of the converter is transferred to three-phase IM using the three-phase VSI. The motor's functioning is subsequently disrupted when the load appears, which is corrected by employing a CFL controller through contrasting the N_{act} and N_{ref}. This controller's output eventually provides through a PWM generator, which generates sufficient pulses for an inverter, and improved output is effectively transmitted to the motor.
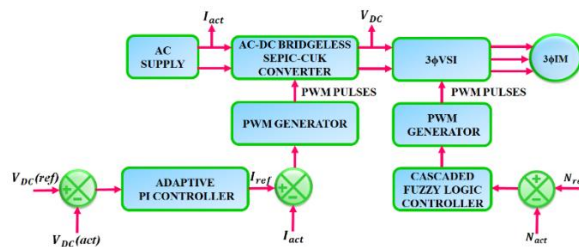

Figure 1. Proposed system

3. MODELLING OF PROPOSED SYSTEM

3.1. Bridgeless AC-DC SEPIC-Cuk converter

Figure 2 depicts the setup of a bridgeless (BL) non-isolated SEPIC-Cuk converter for three-phase IMs. The BL isolated converter operates in continuous state to enable unity power factor functioning at specified constant levels across varied supply voltages. This design is achieved by combining separated Cuk and SEPIC converters that operate in two different half phases. The switch S_1, inductors L_1, L_3 capacitance C_1 and diode D_1 supports the SEPIC converter regulate the current on the positive half phase. Subsequently, the switch S_2 and inductor L_2, capacitance C_2 and diode D_O regulate the current negative half phase during Cuk converter operating mode.
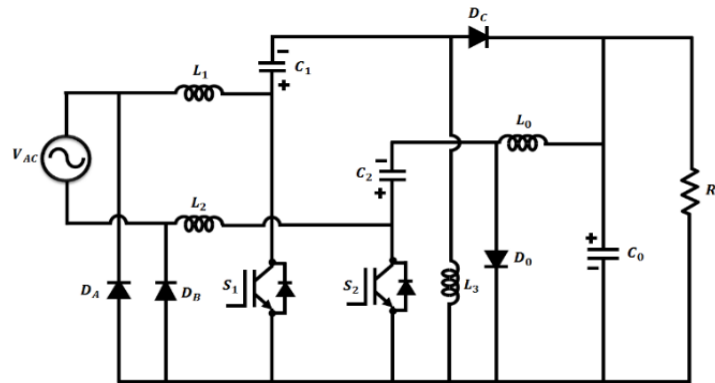

Figure 2. Proposed non-isolated BL SEPIC-Cuk converter

3.1.1. Modes of operation

At the end of each transitioning phase, the architecture of this converter allows for the electrical current through the inductors $L_1, L_2, and\ L_3$ to remain discontinuous. Three separate ways of working along with the key functioning of the suggested non-isolated converter are given in the SEPIC and Cuk phases during two different half phases correspondingly.

- Stage 1 $[t_o - t_1]$

During this state of operation, the switch S_1 gets turned on. If the electrical power of the source is preserved, the current passing through the input inductors L_1 and L_3 steadily rises. The amount of voltage that passes through the power transferring capacitor C_1 is shown in Figure 3(a). During this time, the diode D_c fails to operate.

- Stage 2 $[t_1 - t_2]$

This state starts when switch S_1 gets turned off at moment t_1 as shown in Figure 3(b). The operation is initiated by D_c, the diode output. The stored energy gets released across the capacitor C_1 to the diode D_c, and the current from the inductor lowers at the same slope observed in stage-1.

- Stage 3 $[t_2 - t_3]$

Switches S_1 and S_2 remain turned off at this moment. The current L_3 is lowered because diode current travels through C_O to the load. Figure 3(c) shows the required current passing over capacitor C_1 and the energy discharged through C_O output capacitor when D_c is turned on.

- Stage 4 $[t_3 - t_4]$

In this mode of operation switch S_2 is turned on. The electrical power of the supply is maintained, the amount of electricity passing via the input inductances L_2 constantly rises. As shown in Figure 3(d), the output current in the inductor L_O increases.

- Stage 6 $[t_4 - t_5]$

Both switches are turned off in this stage of operation. As the power of the electrical source is retained, the amount of current flowing via the input inductances L_2 steadily increases. As seen in Figure 3(e), the voltage that flows over the energy transfer capacitor C_2 decreases. At this point, the diode D_c ends operating and stops conducting.

- Phase 6 $[t_5 - t_6]$

As the electrical power of the source is maintained, the quantity of electricity passing via the input inductor L_2 constantly rises. The off condition of the switches continues in this case also. As shown in Figure 3(f), current in the inductor L_O increases. The integration of an adaptive PI controller considerably improves its adaptability properties of the suggested converter.
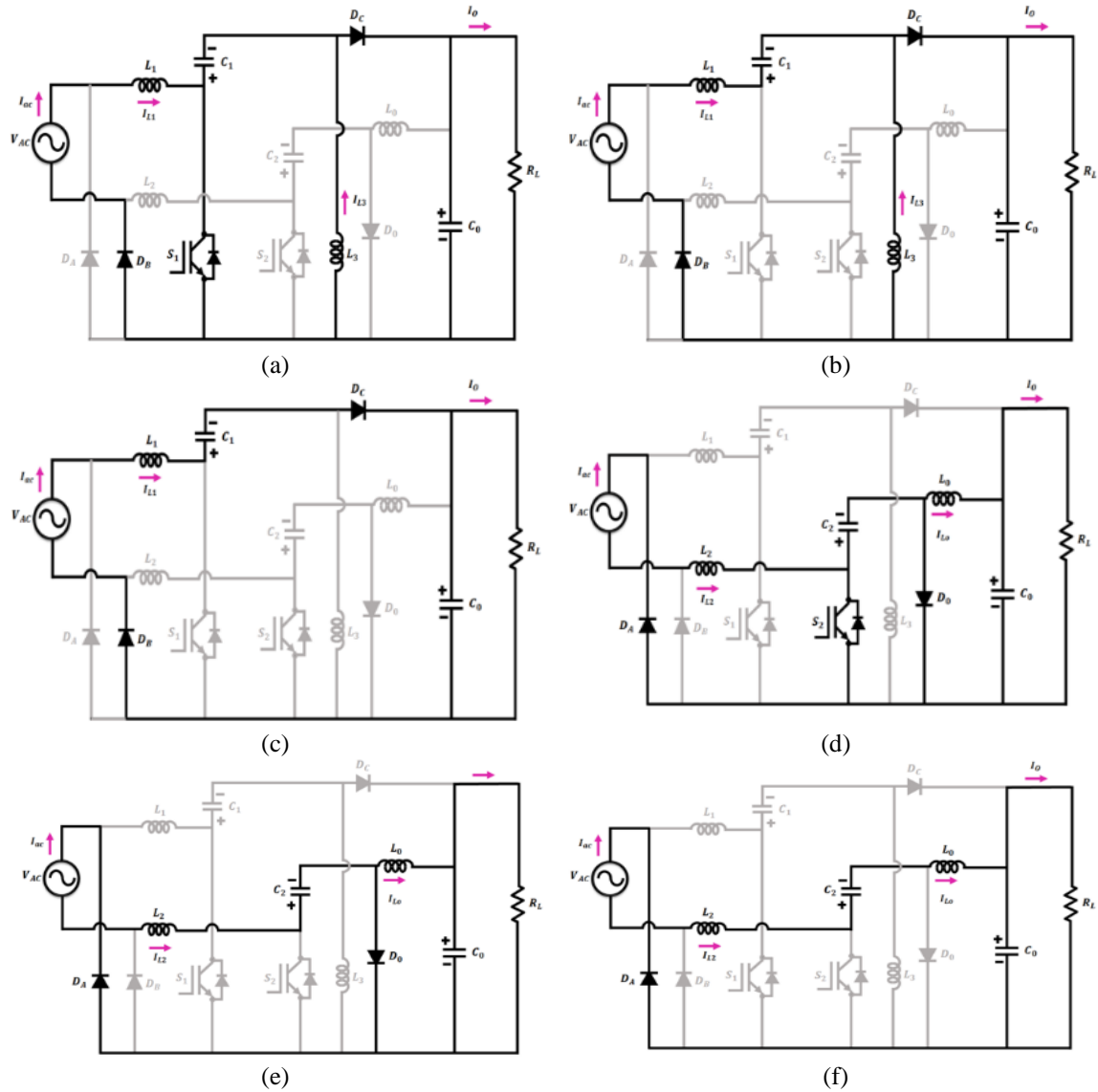
Figure 3. Modes of operations 3: (a) mode 1, (b) mode 2, (c) mode 3, (d) mode 4, (e) mode 5, and (f) mode 6

3.2. Adaptive PI controller

By contrasting reference voltage V_{DC}^* with an actual DC voltage, which is the result of a bridgeless SEPIC-Cuk converter, an adaptive PI controller establishes reference current. By taking into consideration the following equation:

$$\dot{y} = F(x) + G(x).u \qquad (1)$$

The selected control input is:

$$u = G(x)^{-1}[-F(x) + v] \qquad (2)$$

here$= \dot{y}_r - \widehat{K}_P e - \widehat{K}_I \int_0^t edt$, and $y_r = V_{DC}^*$

When employed in a closed-loop regulation equation, the set-point V_{DC}^* denotes the reference DC voltage and is stated as (3).

$$u = G(x)^{-1}\left[-F(x) + \dot{y}_r - \widehat{K}_P e - \widehat{K}_I \int_0^t edt\right] \qquad (3)$$

Where $\hat{K}_P$ and $\hat{K}_I$ are the adaptive PI controller's proportional and integral gains, respectively. $\tilde{K}_I = K_I - \hat{K}_I$ and $\tilde{K}_P = K_P - \hat{K}_P$ are calculation errors of the control variables. By substituting (3) in (1), the resultant equation is (4).

$$\dot{y} = v \tag{4}$$

The DC link voltage of error dynamic is represented by (5).

$$e = y - y_r \tag{5}$$

Differentiating in (5) gives the following solution:

$$\dot{e} = \dot{y} - \dot{y}_r \tag{6}$$

from (4) and (6), it is clear that:

$$\dot{e} = v - \dot{y}_r \tag{7}$$

the expression that results from changing the value of v in the previously mentioned equation is

$$\dot{e} = -\hat{K}_P e - \hat{K}_I \int_0^t e \, dt \tag{8}$$

the suggested adaptive PI controller performs better than the classic PI controller and effectively minimizes the steady state error.

3.3. Cascaded fuzzy logic controller

The implementation of an appropriate controller, such as a CFLC, enables the necessary correction for errors and governs the speed of the IMs motor. Cascaded control is used to assure entire system control and can help with faster reaction times to interruptions. Fuzzy cascade mechanisms were devised and employed for this work because fuzzy sets are excellent at dealing with issues of non-linearity and uncertainty in a system.

The two FLCs are linked in sequence to provide the cascaded control method that has been suggested. The second FLC is driven by reference control signal from the first FLC to produce the appropriate duty cycle ΔD command that regulates the converter's switching pulses. The main aim of the subsequent FLC is to reduce distortions that are harmful for IMs. Figure 4 depicts the CFLC architecture. The converter's voltage output V_o is contrasted with the reference voltage V_{ref} to determine the error E. The CFLC receives the error E as well as the change in error E as input. The following are the main elements that make up the FLC:

- Fuzzifier: A fuzzifier's primary objective is to change the inputs and provide data to the fuzzy inference. Following the definition of the membership functions, the fuzzy subsets $\{PB, PM, PS, Z, NS, NM, and\ NB\}$ are constructed.
- Rule base: The rule basis is developed utilizing information regarding IM motor speed functioning, and it is adjusted in accordance with the findings of the tests. Fuzzy linguistic variables are frequently used for expressing the rule base. The k-th language control rule for the intended 7×7 rule base is provided as:

$$R^k: IF E_k\ is\ A_k\ and\ \Delta E_k\ is\ B_k\ THEN\ U_k = C_k \tag{9}$$

there, the control variable value is given as C_k, the change in error is shown as ΔE_k, the output is considering as U_k, the error is given as E_k, and $k - th\ rule\ (k = 1,2,\ldots,m)$ is given as R^k. Change of error and error are given the linguistic values A_k and B_k, accordingly.

- Interface engine: The inference engine calculates each rule's weighting factor w_K utilising Mamdani's MIN fuzzy implications of the membership degrees $\_\mu_{Ak}(E)\ and\ \mu_{Bk}(\Delta E)$.

$$W_k = min\{\mu_{Ak}(E), \mu_{Bk}(\Delta E)\} \tag{10}$$

The process of making decisions based on a rule base is handled by the inference engine.

The membership functions of E and ΔE are zero (ZO), positive medium (PM) and negative medium (NM), negative small (NS), positive small (PS), negative big (NB), positive big (PB), which are essential to

the system's overall performance. Along with the CFLC rule base, the triangle membership functions of the inputs ΔE and E are also shown in Figure 5(a) and the proposed CFLC rule base is indicated in Figure 5(b).
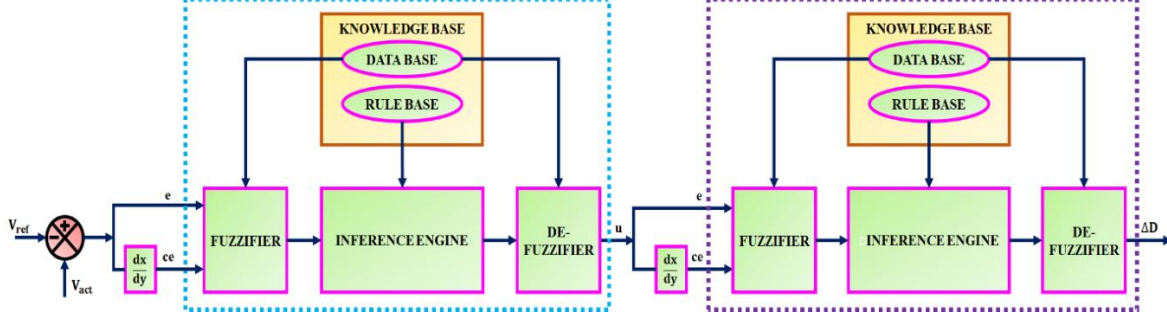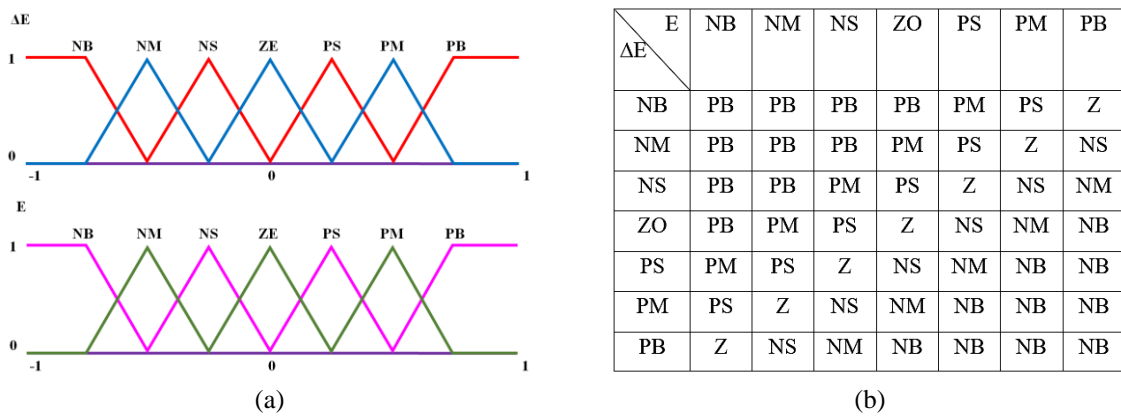

Figure 4. Architecture of CFLC

E $\backslash$ ΔE	NB	NM	NS	ZO	PS	PM	PB
NB	PB	PB	PB	PB	PM	PS	Z
NM	PB	PB	PB	PM	PS	Z	NS
NS	PB	PB	PM	PS	Z	NS	NM
ZO	PB	PM	PS	Z	NS	NM	NB
PS	PM	PS	Z	NS	NM	NB	NB
PM	PS	Z	NS	NM	NB	NB	NB
PB	Z	NS	NM	NB	NB	NB	NB

(a)   (b)

Figure 5. Illustration of CFLC controller (a) triangle membership functions of E and ΔE and (b) rule base

3.4. Modelling of induction motor

A number of parameters are given below as a basis for the computation of IM in a natural abc reference. The electrical balancing calculation for a stator phase of an IM is shown as the following in the abc reference frame:

$$u_A = r_A i_A + \frac{d\psi_A}{dt} \tag{11}$$

Because the stator phase's flux-linkage depends on the rotor's (i_A, i_B, i_C) and stator's (i_a, i_b, i_c)) currents as well as the angle between the appropriate axes, the flux-linkage derivative in (1) is (12).

$$\frac{d\psi_A}{dt} = \frac{\partial\psi_A}{\partial i_A} \cdot \frac{di_A}{dt} + \frac{\partial\psi_A}{\partial i_B} \cdot \frac{di_B}{dt} + \frac{\partial\psi_A}{\partial i_C} \cdot \frac{di_C}{dt} + \frac{\partial\psi_A}{\partial i_a} \cdot \frac{di_a}{dt} + \frac{\partial\psi_A}{\partial i_b} \cdot \frac{di_b}{dt} + \frac{\partial\psi_A}{\partial i_C} \cdot \frac{di_C}{dt} + \frac{\partial\psi_A}{\partial \vartheta} \cdot \frac{d\vartheta}{dt} \tag{12}$$

The dynamic inductances are partial derivatives with regard to currents in (2). A self-inductance of a stator A-phase L_{AA}, mutual inductances between the stator and rotor L_{Aa}, L_{Ab} and mutual inductances between stator phases L_{AB} and L_{AC} and L_{Ac}, respectively, are all static inductances that ignore nonlinearities in the magnetic path of an IM. The item:

$$\frac{\partial\psi_A}{\partial \vartheta} \cdot \frac{d\vartheta}{dt} = \frac{\partial\psi_A}{\partial \vartheta} Z_P \omega \tag{13}$$

A stator's A-phase L_{AA} self-inductance comprises elements from both the coupling and leakage magnetic flux. Considering the inductance of a single phase L_{ms} and inductance of primary magnetic flux for a stator phase L_m.

$$L_m = \frac{3}{2} L_{ms} \tag{14}$$

A comparable ratio for the leaking inductance $L_{\sigma s}$:

$$L_{AA} = \frac{2}{3}(L_m + L_{\sigma s}) \tag{15}$$

where L_m and $L_{\sigma s}$ are the components of an IM's conventional comparable circuit. Given the identical machine and symmetrical power supply, it is clear that an IM can be expressed as an equivalent circuit. When modelling an IM, it is useful to use the analogous circuit's parameters, and the method to accomplish so is simple. According to the presumption of their symmetry, the formula that follows is used to determine the mutual inductance between stator windings:

$$L_{AB} = L_{AC} = L_{AA}\cos\frac{2\pi}{3} = -\frac{1}{3}(L_m + L_{\sigma s}) \tag{16}$$

The mutual inductance L_m among the rotor and stator is being computed for $\vartheta = 0$ whereas the mutual inductances L_{Aa}, L_{Ab} and L_{Ac} between the stator and rotor are variables of the angle.

$$L_{Aa} = \frac{2}{3k}L_m\cos\vartheta$$

$$L_{Ab} = \frac{2}{3k}L_m\cos\left(\vartheta + \frac{2\pi}{3}\right)$$

$$L_{Ac} = \frac{2}{3k}L_m\cos\left(\vartheta - \frac{2\pi}{3}\right) \tag{17}$$

Here, the turn ratio of stator winding with rotor winding is represented by $K = N_r/N_s$. N_r, N_s is no. of rotor and stator windings.

The expression for a stator winding, often known as a rotor phase, is comparable to (11):

$$u_a = r_a i_a + \frac{d\psi_a}{dt} \tag{18}$$

here the expression for the flux-linkage derivative $\frac{d\psi_a}{dt}$ is similar to (12) and includes the self-inductance L_{aa} of a rotor phase, mutual inductances L_{ab}, L_{ac} across rotor windings, and mutual inductances L_{Aa}, L_{Ab}, and L_{Ac} between rotor and stator. Similar to (15), the turn ratio k is utilized to calculate self-inductance of a rotor phase.

$$L_{aa} = \frac{2}{3k^2}(L_m + L_{\sigma r}) \tag{19}$$

Considering the symmetry of the rotor windings, the mutual inductance is:

$$L_{ab} = L_{ac} = L_{aa}\cos\frac{2\pi}{3} = -\frac{1}{3k^2}(L_m + L_{\sigma r}) \tag{20}$$

by enabling concurrent regulation of both frequency and voltage utilizing bridgeless SEPIC-Cuk converter and CFLC, correspondingly, the speed of IM is regulated through keeping a steady voltage.

4.   RESULTS AND CONCLUSION

Hence, this study presents an AC-DC Bridgeless SEPIC-Cuk converter to achieve increased PQ with unity PF. The recommended converter's functioning is regulated by an adaptive PI controller. The implementation of a CFL controller governs the speed of three-phase IM. To maximize its efficacy, the recommended approach is developed using the MATLAB platform and the corresponding waveforms are presented below. Table 1 represents the description parameters of presented model. Similarly, the IM specifications are listed in Table 2.

Figure 6 depicts an illustration of voltage and input current supplied by the AC source. The magnitude of the voltage and current obtained from the alternating current mains is 10 A and 330 V, accordingly. The input AC voltage is provided to bridgeless SEPIC-Cuk converter, according to the Figure 7(a), the constant current 3.8 A is preserved after 0.4 sec with minor distortions. Similarly, the stable voltage 300 V is maintained with less distortions, which is denoted in Figure 7(b).

Table 1. Specifications of converter

Bridgeless SEPIC-Cuk converter	
Parameter	Values
Input AC supply range (V_{AC})	$180 - 270\ V$
Input power rating	$1\ kW$
Output DC voltage range (V_{DC})	$270 - 330\ V$
L_1, L_2	$1\ mH$
L_3, L_O	$3.7\ mH$
C_1, C_2	$47\ \mu F$
C_O	$570\ \mu F$
Diode	$IN4148$
Switch	$IRF840$
Controller	$FPGA\ Spartan\ 6E$
Driver Circuit	$TLP250$

Table 2. Specifications of induction motor

3ϕ Induction motor	
Parameters	Values
Power	$1\ Hp$
Speed	$1390\ rpm$
Voltage	$415\ V\ (AC)$
No. of poles	4
Frequency	$50\ Hz$
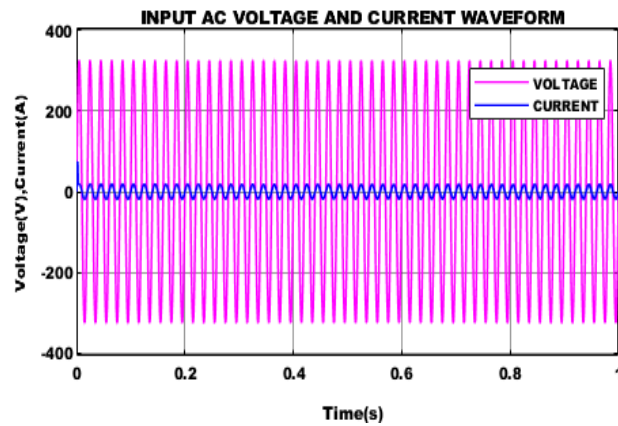
Figure 6. Input AC source current and voltage
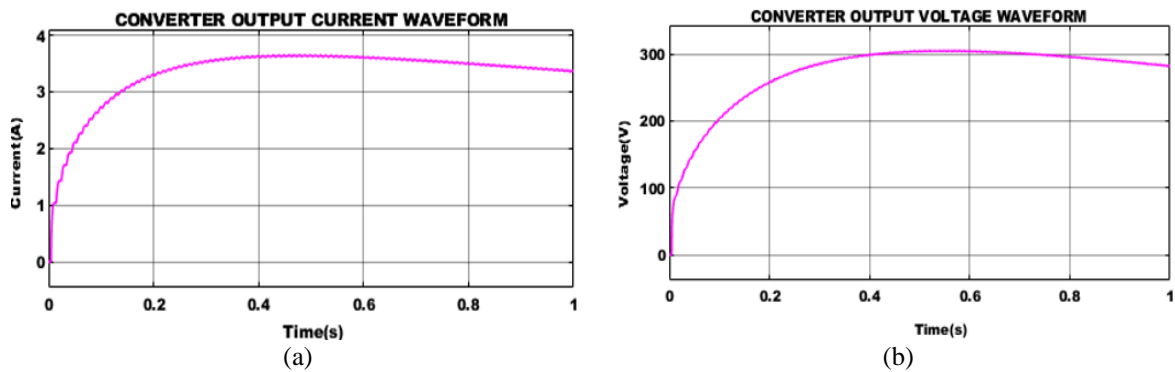
Figure 7. Waveform representation of BL SEPIC-Cuk converter (a) current and (b) voltage

The primary goal of a system of regulation is to keep a constant PF under varying operating circumstances. Figure 8 shows that unity PF is reached promptly at 0.01 s. When a non-isolated bridgeless

SEPIC-Cuk converter is powered by an AC input voltage, a constant and regulated DC link output voltage of 300 V is achieved employing the adaptive PI controller based PWM generator approach as presented in Figure 9. Figure 10 indicates the line-to-line inverter voltage waveform, from observation is it clear that the constant voltage 300 V is attained. According to Figure 11(a), the CFL establishes speed regulation in 0.01 s, whereas the PI controllers require further to achieve a constant speed of 1500 rpm. Likewise in Figure 11(b), the motor current initially increased in amplitude of 2.9 A, then rapidly decreased at 0.2 sec and maintained the constant value 0.98 A at 0.8 sec.
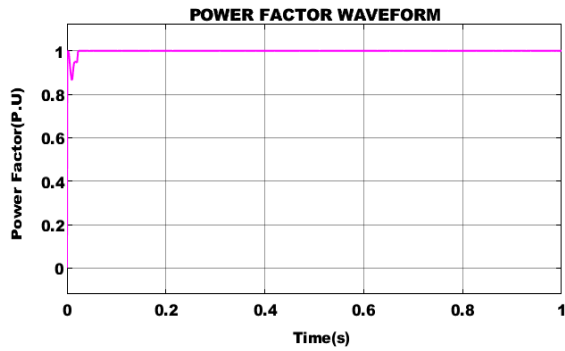
Figure 8. Power factor waveform
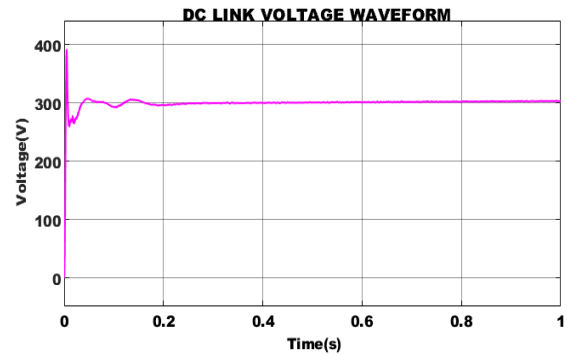
Figure 9. DC link voltage waveform
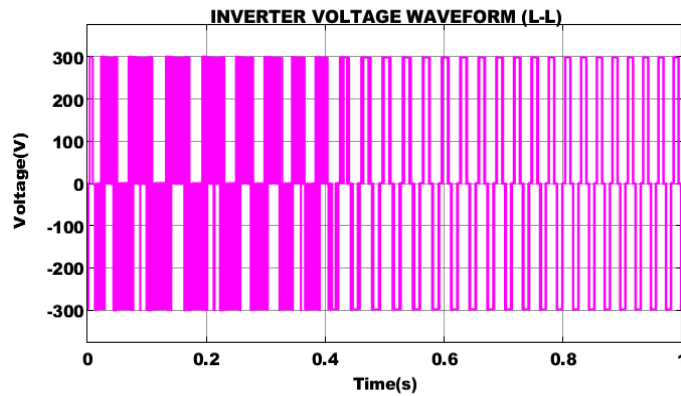
Figure 10. Inverter voltage waveform
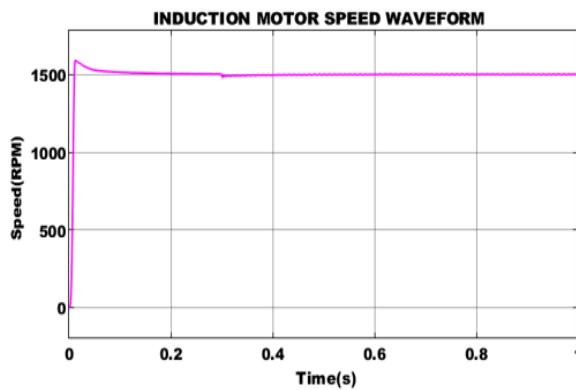
(a)
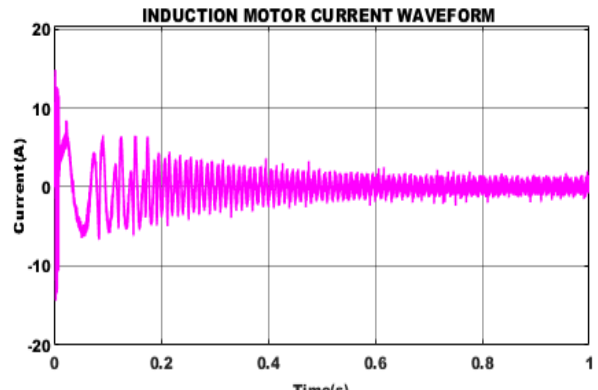
(b)

Figure 11. Three-phase induction motor speed regulation using (a) CFL controller and (b) motor current

The motor load waveform is represented Figure 12(a) the stable value is maintained after 0.3 sec. Figure 12(b) depicts the torque waveform of the three-phase IM. The torque waveform demonstrates that the

utilization of CFL reduces the fluctuations in the beginning phase and makes it steady at 0.4 s. The bridgeless SEPIC-Cuk converter, displayed in Figure 13, obtains a significantly reduced THD value of 2.81%. By reducing THD, power factor correction helps alleviate the stress related issues, extending the operational life of electrical devices. Moreover, THD reduction through power factor correction helps mitigate these voltage distortions, ensuring a stable and reliable power supply.

Table 3 represents the comparison of proposed converter with different BL converter, such as BL-boost [22], BL- Cuk [23], BL-SEPIC [24] and BL-buck boost [25]. The corresponding plots are represented in Figure 14 respectively. By looking at the graph, it is obvious that the suggested BL SEPIC-Cuk converter has a high efficiency value of 96.8% and a low THD value of 2.81%.

(a)   (b)
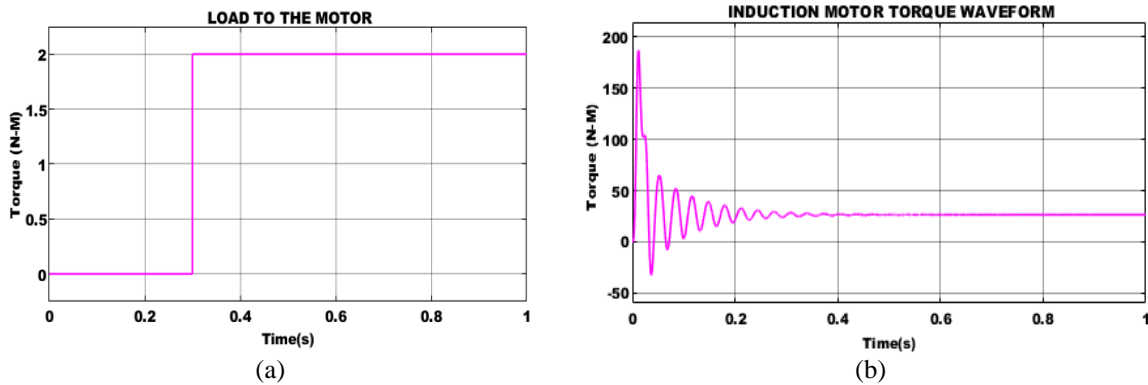
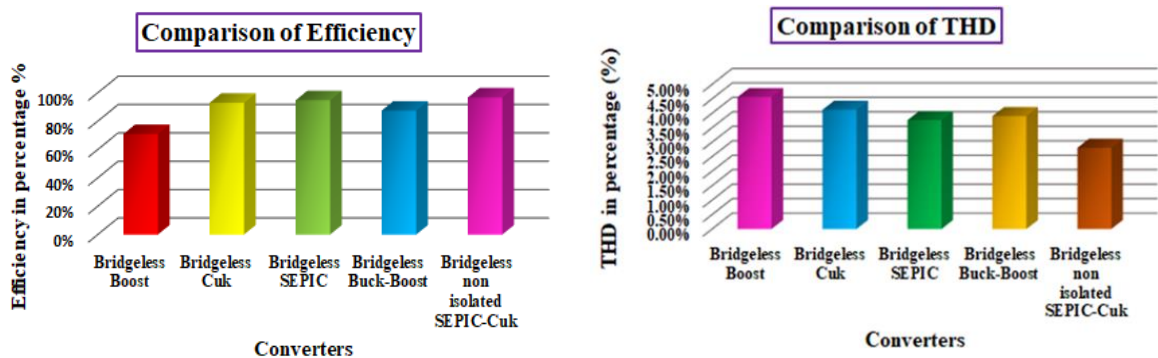Figure 12. Motor waveforms (a) motor load and (b) torque waveform of IM
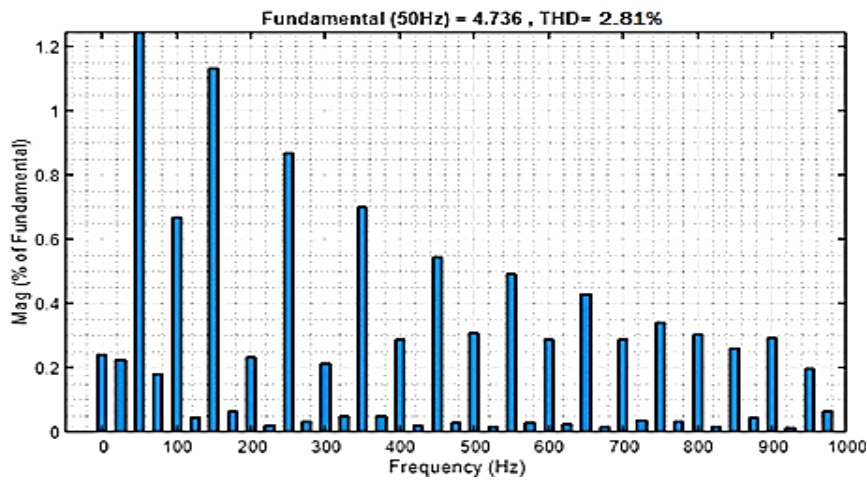
Figure 13. THD waveform

Figure 14. Comparison analysis of efficiency and THD

Table 3. Comparison analysis of efficiency

Converters	Efficiency%
Bridgeless boost [22]	71%
Bridgeless Cuk [23]	93%
Bridgeless SEPIC [24]	94.8%
Bridgeless SEPIC-boost [25]	87.5%
Bridgeless non isolated SEPIC-Cuk	96.8%

5. CONCLUSION

To address the power quality issues, this research develops an AC-DC bridgeless SEPIC-Cuk converters, the power quality at the input AC supply side has been improved and the converter has excellent dependability with less switching stress. The adaptive PI controller is implemented in this paper to preserve a steady DC link voltage with low fluctuations. The switching functionality of the three-phase VSI is regulated by the CFL controller, which also controls the speed of the three-phase IM. Implementing the recommended control method improves power quality by lowering THD considerably. The system that has been proposed is simulated in the MATLAB platform, and the results show that the proposed system is extremely has maximum efficiency value of 96.8% with a reduced THD value of 2.81%.

REFERENCES

[1] M. Gonzalez-Ramirez and C. A. Cruz-Villar, "Variable speed drive with PFC front-end for three-phase induction motor," *Electronics Letters*, vol. 53, no. 16, pp. 1139–1140, Aug. 2017, doi: 10.1049/el.2017.1671.
[2] S. Arunraj, S. Murugesan, T. U. Nandhini, and K. Keerthana, "A Novel Zeta Converter with Pi Controller for Power Factor Correction in Induction Motor," *Ijsrst*, vol. 3, no. 8, pp. 230–234, 2017.
[3] V. B. M. Krishna and S. Vuddanti, "Identification of the best topology of delta configured three phase induction generator for distributed generation through experimental investigations," *International Journal of Emerging Electric Power Systems*, vol. 23, no. 3, pp. 329–341, 2022, doi: 10.1515/ijeeps-2021-0064.
[4] S. S. Duvvuri, V. Sandeep, K. Yadlapati, and V. B. M. Krishna, "Research on induction generators for isolated rural applications: State of art and experimental demonstration," *Measurement: Sensors*, vol. 24, 2022, doi: 10.1016/j.measen.2022.100541.
[5] A. S. Omran, N. H. Abbasy, and R. A. Hamdy, "Enhanced performance of substation dynamics during large induction motor starting using SVC," *Alexandria Engineering Journal*, vol. 57, no. 4, pp. 4059–4070, 2018, doi: 10.1016/j.aej.2018.10.009.
[6] M. Banagar and A. Usha, "Design and simulation of bridgeless PFC buck boost converter fed BLDC motor drive," *2017 Innovations in Power and Advanced Computing Technologies, i-PACT 2017*, vol. 2017-January, pp. 1–7, 2017, doi: 10.1109/IPACT.2017.8244880.
[7] S. Saini, P. Sharma, D. K. Dhakad, and L. K. Tripathi, "Power Factor Correction Using Bridgeless Boost Topology," *International Journal of Advanced Engineering Research and Science*, vol. 4, no. 4, pp. 209–215, 2017, doi: 10.22161/ijaers.4.4.32.
[8] B. N. Kommula and V. R. Kota, "PFC based SEPIC converter fed BLDC motor with torque ripple minimization approach," *2017 International Electrical Engineering Congress, iEECON 2017*, 2017, doi: 10.1109/IEECON.2017.8075743.
[9] J. Rajesh, S. Shobana, and K. Somasekar, "Bridgeless Sepic converter for reduction of ripple current and conduction loss," vol. 8, pp. 166–173, 2018.
[10] A. Dixit, K. Pande, S. Gangavarapu, and A. K. Rathore, "DCM-Based Bridgeless PFC Converter for EV Charging Application," *IEEE Journal of Emerging and Selected Topics in Industrial Electronics*, vol. 1, no. 1, pp. 57–66, 2020, doi: 10.1109/jestie.2020.2999595.
[11] Z. Chen, P. Davari, and H. Wang, "Single-Phase Bridgeless PFC Topology Derivation and Performance Benchmarking," *IEEE Transactions on Power Electronics*, vol. 35, no. 9, pp. 9238–9250, 2020, doi: 10.1109/TPEL.2020.2970005.
[12] G. E. Mejía-Ruiz, N. Muñoz-Galeano, and J. M. López-Lezama, "Modeling and development of a bridgeless PFC Boost rectifier," *Revista Facultad de Ingeniería Universidad de Antioquia*, vol. 82, pp. 9–21, Mar. 2017, doi: 10.17533/udea.redin.n82a02.
[13] X. Lin, Z. Jin, F. Wang, and J. Luo, "A Novel Bridgeless Cuk PFC Converter with Further Reduced Conduction Losses and Simple Circuit Structure," *IEEE Transactions on Industrial Electronics*, vol. 68, no. 11, pp. 10699–10708, 2021, doi: 10.1109/TIE.2020.3031527.
[14] J. Kim, S. Han, W. Cho, Y. Cho, and H. Koh, "Design and analysis of a repetitive current controller for a single-phase bridgeless sepic pfc converter," *Energies*, vol. 12, no. 1, 2019, doi: 10.3390/en12010131.
[15] M. Kavitha and V. Sivachidambaranathan, "Power factor correction in fuzzy based brushless DC motor fed by bridgeless buck boost converter," *6th International Conference on Computation of Power, Energy, Information and Communication, ICCPEIC 2017*, vol. 2018-January, pp. 549–553, 2017, doi: 10.1109/ICCPEIC.2017.8290426.
[16] X. Lin and F. Wang, "New Bridgeless Buck PFC Converter with Improved Input Current and Power Factor," *IEEE Transactions on Industrial Electronics*, vol. 65, no. 10, pp. 7730–7740, 2018, doi: 10.1109/TIE.2018.2801782.
[17] M. M. Kamble, "Simulation and Performance Analysis of SEPIC (DC-DC) Converter using Genetic Algorithm based PI Controller Full bridge rectifier S1," *International Research Journal of Engineering and Technology (IRJET)*, vol. 07, no. 09, pp. 2068–2072, 2020.
[18] M. Sivaramkrishnan, M. S. Ramkumar, S. Subramanian S, and N. S. D. Ladu, "A Bridgeless LUO Converter with Glowworm Swarm Optimized Tuned PI Controller for Electrical Applications," *Mathematical Problems in Engineering*, vol. 2022, 2022, doi: 10.1155/2022/2401261.
[19] H. C. Mohanta *et al.*, "An Optimized PI Controller-Based SEPIC Converter for Microgrid-Interactive Hybrid Renewable Power Sources," *Wireless Communications and Mobile Computing*, vol. 2022, 2022, doi: 10.1155/2022/6574825.
[20] I. Sudiharto, Y. C. Arif, H. Eko H.s., F. D. Murdianto, and A. T. Prasetyo, "Design and implementation SEPIC converter using pi controller for solution power quality improvement," *Proceedings - 2019 5th International Conference on Science and Technology, ICST 2019*, 2019, doi: 10.1109/ICST47872.2019.9166349.

[21] S. S. Deekshit, R. M. Mohan, and C. V. Reddy, "A power quality improved bridgeless converter based computer power supply by using fuzzy logic controller," *International Journal of Electrical Engineering*, vol. 10, no. 2, pp. 197–221, 2017.
[22] H. Wang, Y. Tang, and A. Khaligh, "A bridgeless boost rectifier for low-voltage energy harvesting applications," *IEEE Transactions on Power Electronics*, vol. 28, no. 11, pp. 5206–5214, 2013, doi: 10.1109/TPEL.2013.2242903.
[23] A. A. Fardoun, E. H. Ismail, A. J. Sabzali, and M. A. Al-Saffar, "New efficient bridgeless cuk rectifiers for PFC applications," *IEEE Transactions on Power Electronics*, vol. 27, no. 7, pp. 3292–3301, 2012, doi: 10.1109/TPEL.2011.2182662.
[24] J. W. Yang and H. L. Do, "Bridgeless sepic converter with a ripple-free input current," *IEEE Transactions on Power Electronics*, vol. 28, no. 7, pp. 3388–3394, 2013, doi: 10.1109/TPEL.2012.2226607.
[25] B. Zhao, A. Abramovitz, and K. Smedley, "Family of Bridgeless Buck-Boost PFC Rectifiers," *IEEE Transactions on Power Electronics*, vol. 30, no. 12, pp. 6524–6527, 2015, doi: 10.1109/TPEL.2015.2445779.

BIOGRAPHIES OF AUTHORS

R. Suguna is a Ph.D. student, who received a bachelor's degree in Electrical and Electronics Engineering from Anna University in 2006 and the Master's degree in Power Electronics and Industrial Drives from Sathyabama University in 2010. Fields of interest is computational intelligence, transient analysis, and machine drives. She has published more than 15 papers in international journals. She can be contacted at email: rsuguna016@gmail.com.

Dr. S. Tamil Selvi has been an Associate Professor of Electrical and Electronics Engineering at SSN College of Engineering in Tamil Nadu, India, since 2016. She received a B.E. degree with First Class in Electrical and Electronics Engineering and an M.E. degree with First Class Distinction in Power System Engineering from Madurai Kamaraj University in Madurai, India, in 1999 and 2002, respectively. She successfully completed her Ph.D. (full time) in distribution transformer design using evolutionary algorithms at Anna University in 2015. She has a GATE score of 85.53 percentile. She has 19 years of work experience, including 13 years teaching, 2 years in industry, and 4 years of full-time research. She has worked at various institutions, including Sri Venkateswara College of Engineering, K.L.N. College of Engineering, St. Joseph's College of Engineering, Tagore Engineering College, Adhiparasakthi Engineering College, and On Spec Legend Information Systems. Her research has been published in 15 Science Citation-indexed international journals. She has four chapters and two books published. In order to assist the research community, she has also released her software code for NSGA-II, a multi-objective evolutionary algorithm, on "MATLAB Central." Her area of interest is the application of evolutionary algorithms to transformer design, power system operation, and optimization problems. She can be contacted at: tamilselvis@ssn.edu.in.

Dr. K. Mohana Sundaram received a B.E. degree in Electrical and Electronics Engineering from the University of Madras in 2000, M.Tech. degree in High Voltage Engineering from SASTRA University in 2002 and a Ph.D. degree from Anna University, India in 2014. His research interests include intelligent controllers, power systems, embedded systems, and power electronics. He has completed a funded project of worth Rs.30.79 lakhs sponsored by DST, Government of India. Currently he is working as a professor in the EEE department at the KPR Institute of Engineering and Technology, India. He has produced eight Ph.D. candidates under his supervision at Anna University, Chennai. He has published six books and serves as a reviewer for IEEE, Springer, and Elsevier journals. He is an active member of IEEE, IE, ISTE, and IAENG. He has published around 74 papers in international journals. He can be contacted at email: kumohanasundaram@gmail.com.

Pradeep Katta received a B.Tech. degree in Electrical and Electronics Engineering from Gokula Krishna College of Engineering in 2008 and M.E. degree in Embedded System Technologies from Veltech in the year 2010. Currently working as an assistant professor at Veltech Hightech Dr Rangarajan Dr Sakunthala Engineering College, Chennai. His field of interest is electrical machines and power quality. He has published more than 15 papers in international journals. He can be contacted at email: pradeep.2048@gmail.com.